Simple Robust Model Predictive Current Control for PMSM Drives Without Flux-Linkage Parameter

Xiaoguang Zhang, *Senior Member, IEEE*, and Ziwei Wang

***Abstract*—The model predictive control (MPC) has its superiorities in simple algorithm and exceptional dynamic performance. However, the mismatch of the model parameters will strongly affect the control performance on MPC and will also cause current error in prediction. Aiming to enhance the robustness of MPC while eliminating the predicted current error under parameters mismatch, in this article, a simple robust MPC method is put forward. In the proposed control strategy, accurate inductance information can be extracted simply by designing a discrete integral controller based on the predicted current error of the *d*-axis. Moreover, two methods are proposed to deduce the gain coefficient of the integration controller theoretically. Furthermore, in the new current prediction model, the flux-linkage parameter has been replaced by the extracted accurate inductance information. This indicates that the flux-linkage parameter has been removed from the model of current prediction. Since the resistance does not have much influence on the accuracy of the current prediction model, the inductance parameter becomes the only factor that predominantly affects the accuracy of the current prediction model. Finally, the experimental results prove the effectiveness of the proposed method.**

***Index Terms*—Model predictive control (MPC), permanent magnet synchronous motor (PMSM), robustness.**

I. Introduction

PERMANENT magnet synchronous motor (PMSM) has been used in various industrial occasions deal to its excellent features of small size, fast response, and high efficiency [1]–[3]. The well-known control strategies, which are the research hotspot applied to the PMSM, are field-oriented control (FOC) [4], direct torque control (DTC) [5], and model predictive control (MPC) [6]. In these control strategies, FOC is extensively used in industrial applications by reason of its simplicity and good performance [7]. DTC has its unique advantages in terms of the fast response on torque performance [8].

Over the past few years, with the advancement of the digital signal processors and the capacity of the chip storage, the MPC that is based on a mathematical model has become a new research hotspot gradually. The MPC method uses a discrete model to predict the performance of the controlled system in the next control period. Then, according to the requirements of control objectives, the cost function is constructed to compute the results of each vector when they are acting on the control system, respectively. On the basis of the effect of the cost function, the optimal voltage vector or optimal combination of voltage vectors is chosen from the basic voltage vectors [9]. The MPC method has the superiorities of the simple control structure and excellent dynamic performance [10].

MPC method consists of model predictive torque control (MPTC) and model predictive current control (MPCC) [11]–[13]. The strategy of MPTC demands simultaneous consideration of the prediction and control of torque and flux linkage in the motor system. Therefore, to achieve excellent control performance, the cost function in MPTC must design an appropriate weighting factor to counterpoise the torque and flux linkage. The MPCC method is more concise than the MPTC method, as it requires only the control of the current. Therefore, on account of the control variables that have the same dimension in the cost function of the MPCC, weighting factors in the MPTC are avoided in the MPCC strategy.

However, the conventional MPCC method encompasses the motor parameters (stator inductance, stator resistance, and flux linkage) within the model for prediction. The exactness of the model parameters will affect the control performance and the running state of the whole system. In other words, inaccurate model parameters will influence the prediction result and further lead to the wrong vector selection. It can clearly observe that the control performance of the MPCC method will exacerbate significantly under the variation or mismatch in the motor parameters [14].

For the purpose of solving the adverse impact of the mismatch in the model parameters on the performance of prediction control, some investigators had put some excellent methods forward. One way is to set up a parameter disturbance observer. In the literature [15], a stator current and disturbance observer (SCDO) with deadbeat predictive current control (DPCC) was presented

Manuscript received 22 December 2021; revised 14 April 2022; accepted 8 May 2022. Date of publication 25 May 2022; date of current version 12 December 2022. This work was supported in part by the National Natural Science Foundation of China under Grant 51877002, in part by China Postdoctoral Science Foundation funded project under Grant 2021M690601, in part by the 2019 Beijing Nova Program under Grant Z191100001119036, and in part by Jiangsu Planned Projects for Postdoctoral Research Funds under Grant 2021K210B. *(Corresponding author: Xiaoguang Zhang.)*

The authors are with the North China University of Technology (Inverter Technologies Engineering Research Center of Beijing), Beijing 100144, China (e-mail: zxg@ncut.edu.cn; wangziwei130@ncut.edu.cn).

Color versions of one or more figures in this article are available at https://doi.org/10.1109/TIE.2022.3176288.

Digital Object Identifier 10.1109/TIE.2022.3176288

and used in the PMSM system to decrease the effect of the mismatch of the motor parameters. The estimated parameter disturbances are extracted by the SCDO and the DPCC predicts the voltage of the *dq*-axes applied to the space vector pulsewidth modulation. In addition, the literature [16] established the extended state observer to make the whole system be strengthened in terms of its robustness, and at the same time, the entire system adopted an incremental current prediction model, which does not need to consider the impact of the mismatch of the flux linkage. The literature [17] points out a novel observation method that the parameter disturbance of the *dq*-axes current and the speed is capable of being estimated by the high-order sliding-mode observer. This method cooperates with sliding-mode control and can enhance the robustness characteristic of the entire system. These methods mentioned above can observe and compensate for the error caused by any parameter mismatches in the motor, but accurate values of every model parameter cannot be obtained.

Recently, other methods have been published to reduce the parameter sensitivity of MPC. The literature [18] proposed a method that can, respectively, use the current difference in the *dq*-axes to predict the optimal vector to act on the prediction model to achieve the robustness of the entire system. In the literature [19], a strategy is proposed to recompense for the voltage deviation resulting from parameter mismatch through an online calculation module. This method can effectively advance the robustness of the entire system. The literature [20] leads to an update mechanism that can calculate the compensation factor, which is used in the current prediction to get rid of the current error resulting from the mismatch of the model parameters. On the other hand, some other excellent methods of online parameter identification, such as extended Kalman filter [21] and neural network [22], also can make the MPC less sensitive to parameters. However, the perplex calculation procedure among these methods would exacerbate the cumbersome predictive control process. This indicates that the problem of parameter sensitivity of the method of MPC cannot be overcome without increasing structural complexity.

To balance the parameter robustness and structural complexity of MPC, this article puts forward a simple robust MPCC method. In this method, the difference value between the accurate inductance and the model inductance can be extracted by the simple inductance integral extraction controller. And the information of the flux linkage can be replaced by the extracted inductance information of different instants. Therefore, a new current prediction model that eliminates the flux-linkage parameter is proposed.

The rest of this article is organized as follows. First, Section II presents the principle of the MPCC. Then, the parameters sensitivity of the MPCC is analyzed in Section III. In Section IV, algorithms for extracting inductance and calculating flux linkage are proposed. The proposed method is confirmed efficient in Section V. Finally, Section VI concludes this article.

II. Principle of MPCC Method

A. Voltage Equation of PMSM

The SPMSM drive system fed by a two-level converter is used in this article, as shown in Fig. 1.

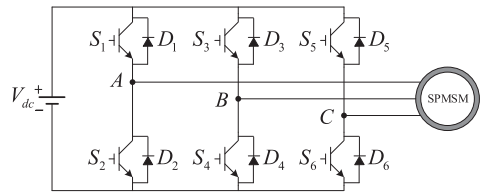

Fig. 1. Two-level inverter SPMSM drive system.

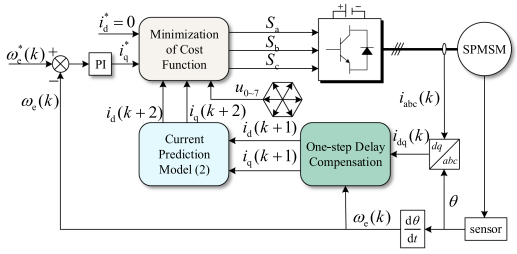

Fig. 2. System control structure of MPCC.

Under the synchronous rotating coordinate system, the mathematical model of PMSM is shown by

$$\begin{cases} u_d = R \cdot i_d + L_d \cdot \frac{di_d}{dt} - \omega_e \cdot L_q \cdot i_q \\ u_q = R \cdot i_q + L_q \cdot \frac{di_q}{dt} + \omega_e \cdot L_d \cdot i_d + \omega_e \cdot \psi_f \end{cases} \tag{1}$$

where u_d and u_q represent the voltages of the d-axis and q-axis, respectively, and i_d and i_q represent the currents of the d-axis and q-axis, respectively. R is the winding resistance. ω_e is the electrical angular velocity (rad/s). ψ_f stands for the flux linkage; L_d and L_q are the stator inductances of the dq-axes, respectively. In this article, the SPMSM is used; thus, the inductance of the d-axis L_d equals the inductance of the q-axis L_q, i.e., $L = L_d = L_q$.

B. Conventional MPCC Method

Fig. 2 illustrates the control diagram of the MPCC method. The reference current of the d-axis is set to 0 and the reference current of the q-axis is determined from the output of the speed-loop proportional integral (PI) controller.

For the prediction of current at the next instant, it is necessary to discretize the voltage Equation (1) by using the first-order Euler method; the expression for the discretized current prediction equation is as follows:

$$\begin{bmatrix} i_d^p(k+1) \\ i_q^p(k+1) \end{bmatrix} = \begin{bmatrix} i_d(k) & i_q(k) & u_d(k) & 0 \\ i_q(k) & -i_d(k) & u_q(k) & -1 \end{bmatrix} \cdot \begin{bmatrix} A & B & T/L & C \end{bmatrix}^T \tag{2}$$

where $A = 1 - TR/L$, $B = T\omega_e$, and $C = T\omega_e\psi_f/L$. $i^p{}_d(k+1)$ and $i^p{}_q(k+1)$ are the predicted currents at $k+1$ instant. T stands for the control period. $u_d(k)$ and $u_q(k)$ are the voltage components on the dq-axes of the selected vector.

Eight basic vectors can be emerged by the two-level voltage source inverter, including six nonzero vectors and two zero vectors. A single basic vector is chosen as the optimal voltage vector in each control period under the MPCC method. Thus, the cost function of the current error is constructed necessarily to assess the control effect of each voltage vector. The cost function

of the error of prediction current can be shown by

$$g = (i_d^* - i_d)^2 + (i_q^* - i_q)^2 \tag{3}$$

where i_d^* and i_q^*, respectively, represent the current reference values of the d-axis and q-axis. i_d and i_q stand for the predictive currents by the influence of the basic vector. Then, in the next control period, the voltage vector with the lowest cost function will be selected as the optimal voltage vector.

III. Analyze the Sensitivity of Parameters in MPCC

The controlling performance of the strategy in MPCC depends critically on the precise parameters of the prediction model [18]. It is shown from (2) in Section II that the current prediction model involves motor parameters (R, L, and ψ_f). If the actual motor parameters cannot match the parameters utilized in the prediction model, the accuracy of the prediction current in the dq-axes will be affected. Furthermore, the result of the cost function (3) will be affected, which will cause the selected vector is not the optimal vector needed by the system.

Therefore, the MPCC needs to be analyzed in terms of its parameter sensitivity. The resistance, inductance, and flux-linkage parameters of the prediction model in this article are represented by R, L, and ψ_f, respectively. In addition, R_0, L_0, ψ_{f0} represent the actual parameters of the motor, i.e., accurate parameters. ΔR, ΔL, and $\Delta\psi_f$ represent the parameter errors. The relationships during the prediction model parameters, the actual parameters, and the parameter errors are revealed as follows:

$$\begin{cases} R_0 = R + \Delta R \\ L_0 = L + \Delta L \\ \psi_{f0} = \psi_f + \Delta\psi_f \end{cases}. \tag{4}$$

Inaccurate prediction model of the dq-axes current can be proved in (2) in which R, L, and ψ_f represent the parameters under interference and $ip\ d\ (k+1)$ and $ip\ q(k+1)$ stand for the inexact currents in prediction, resulting from mismatched parameters.

On the other hand, on the foundation of the actual parameters, the correct current prediction model of the dq-axes is represented by

$$\begin{bmatrix} i_{df}(k+1) \\ i_{qf}(k+1) \end{bmatrix} = \begin{bmatrix} i_d(k) & i_q(k) & u_d(k) & 0 \\ i_q(k) & -i_d(k) & u_q(k) & -1 \end{bmatrix} \cdot \begin{bmatrix} D & B & T/L_0 & E \end{bmatrix}^T \tag{5}$$

where $D = 1 - TR_0/L_0$, $E = T\omega_e\psi_{f0}/L_0$, and $i_{df}(k+1)$ and $i_{qf}(k+1)$ stand for the accurate prediction current of the d-axis and q-axis, respectively.

Therefore, the current prediction errors of the d-axis and q-axis between the prediction current under the exact parameters (5) and the prediction current under the inexact parameters (2) are represented as follows:

$$\begin{aligned} \begin{bmatrix} E_d \\ E_q \end{bmatrix} &= \begin{bmatrix} i_{df}(k+1) - i_d^p(k+1) \\ i_{qf}(k+1) - i_q^p(k+1) \end{bmatrix} \\ &= \begin{bmatrix} i_d(k) & -u_d(k) & 0 \\ i_q(k) & -u_q(k) & 1 \end{bmatrix} \cdot \begin{bmatrix} F & G & H \end{bmatrix}^T \end{aligned} \tag{6}$$

where $F = (TR\Delta L - TL\Delta R)/[L(L+\Delta L)]$, $G = (T\Delta L)/[L(L+\Delta L)]$, and $H = (T\omega_e\psi_f\Delta L - T\omega_e\Delta\psi_f L)/[L(L+\Delta L)]$. Equation (6) proves that mismatched parameters will bring about errors of E_d and E_q in predicting the current.

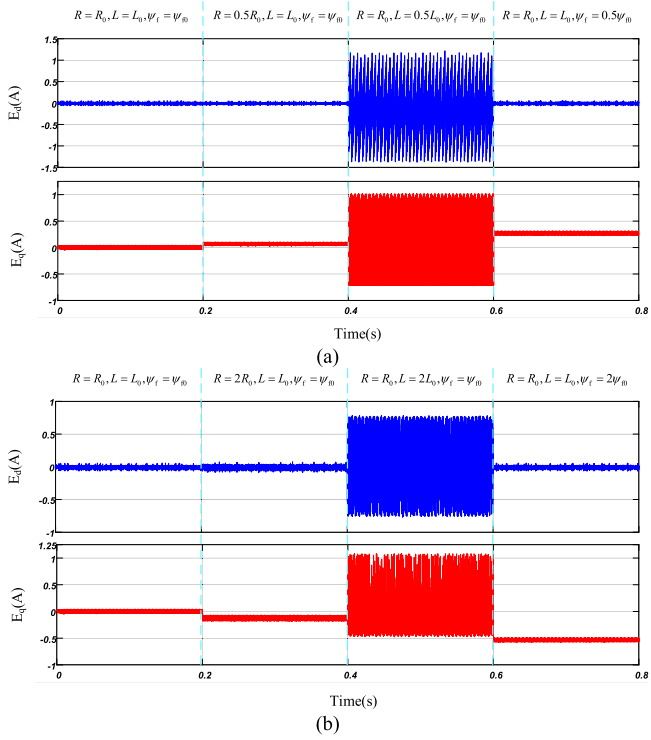

Fig. 3. Results of simulation of E_d and E_q under the influence of different parameters in the MPCC method (The running speed is 1000 r/min, the bus voltage is 310 V, and the control period is 6.7×10^{-5} s). (a) Parameters suddenly decrease by 50%. (b) Parameters suddenly increase by 100%.

TABLE I
Parameters of SPMSM

Motor Parameter Item/Symbol/Unit	Value
Stator resistance/R/Ω	3.18
Stator inductance/L/mH	8.5
Magnet flux linkage/ψ_f/Wb	3.25×10^{-1}
Number of pole pairs/P	2
Rotational inertia/J/kg.m^2	4.6×10^{-4}
Rated load torque/T_{el}/N.m	5
Motor speed /N/r/min	2000
Control period/T/s	6.7×10^{-5}
DC Voltage/V_{DC}/V	310

For the purpose of certifying the concrete effects of the parameters applied to the model (resistance, inductance, and flux linkage), this article conducts a simulation, and the results are displayed in Fig. 3. As the prerequisite of the simulation, the motor parameter values utilized in the prediction model would alter by various intervals of time. In the simulation, accurate parameters of SPMSM are noted in Table I.

Obviously, Fig. 3 is indicative of the fact that there are few errors in the present prediction current when the parameters (the stator resistance, the stator inductance, and the flux linkage) are exact. Resistance mismatch does not significantly affect the current prediction error when it occurs. The reason which can

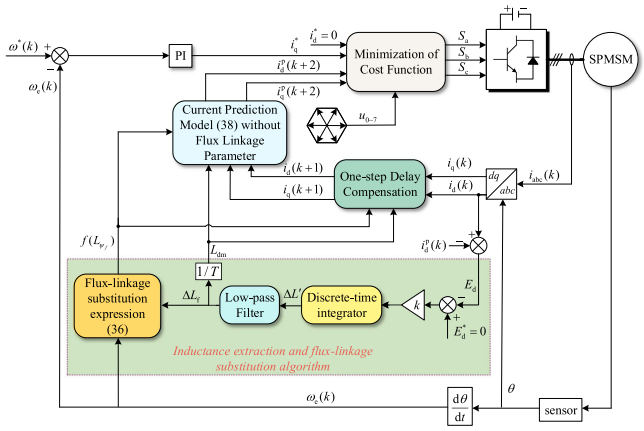

Fig. 4. Control block diagram of robust MPCC model system.

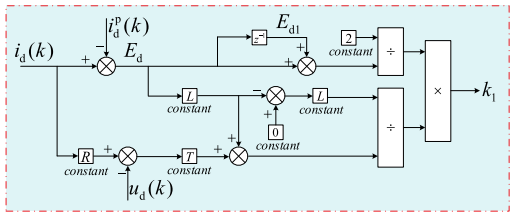

Fig. 5. Diagram of parameter k_1 acquisition.

explain the phenomenon above is that, in the prediction model of current, i.e., (2), only the part *TR/L* is related to the resistance. Because the control cycle of the entire system is so short that the part $TR/L<<1$. Thus, the resistance error has a minimal impact on the current prediction, so it is insignificant enough to be ignored.

It can also be shown in Fig. 3 that there are drastic changes in the current prediction error of E_d and E_q if there is a mismatch between the inductance parameters. On the other hand, when flux-linkage parameters are mismatched, the current prediction error of the q-axis E_q generates a significant variation. In contrast, the current prediction error of the d-axis E_d is not so much affected.

The results above demonstrate that inaccurate resistance parameters do not have a noticeable effect on the prediction current, and the accurate parameter of the inductance is the only factor that impacts the d-axis prediction current. However, the predictive current of the q-axis is affected by inductance precision and flux-linkage accuracy.

IV. Proposed Robust MPCC Method

For the purpose of reducing the errors, which resulted from the mismatched parameters, and strengthen the control performance of the MPCC strategy, an effective strategy based on the conventional MPCC strategy is proposed in this section. Inductance information can be observed in real time by this proposed method. Moreover, the parameter of flux linkage in the predictive model is removed by inductance information and measured current of different control instants. The proposed approach is illustrated in Fig. 4, which shows a diagram of the control flow.

A. Inductance Extraction Algorithm

Based on (6), the error of current prediction in the d-axis E_d is shown by $E_d = -(T \cdot \Delta L)/[L \cdot (L + \Delta L)] \cdot u_d(k)$ since $i_d = 0$ control is applied. Inductance information is evidently incorporated into E_d. Therefore, this section introduces a simple integral inductance extraction method derived from E_d to obtain the accurate inductance parameter.

As shown in Fig. 4, the inductance information can be determined by the integrator of the difference between the actual error of current prediction in the d-axis (E_d) and the reference error of current prediction in the d-axis (E_d^*). Moreover, such as PI controller, the magnitude of the gain factor k in the inductance extraction system needs to be determined. Therefore, two different gain design methods are presented in this article, i.e., *Inductance discretization calculation* and *Laplace transform simplification.*

1) Inductance Discretization Calculation Method: Since the mismatch of the resistance parameter can be neglected, E_d in (6) can be simplified as

$$E_d = i_{df}(k+1) - i_d^p(k+1) = T \cdot [R \cdot i_d(k) - u_d(k)] \cdot [1/(L + \Delta L) - 1/L]. \tag{7}$$

In addition, the inductance error information between the accurate inductance parameter and inductance parameter in the current prediction model can be extracted by integrating the difference between E_d and E_d^*. At the same time, E_d^* is set as 0. Therefore, the parameter that is being integrated is only the E_d, and the following equation can express inductance error information as:

$$\Delta L = k_1 \cdot \int E_d dt. \tag{8}$$

On the basis of (7) and (8), E_d can be further described as

$$E_d = T \cdot [R \cdot i_d(k) - u_d(k)] \cdot \left[\frac{1}{L + k_1 \cdot \int E_d dt} - \frac{1}{L}\right]. \tag{9}$$

Moreover, in order to simplify the calculation, the part of the integral is simply discretized as

$$\int E_d dt = \frac{1}{2}(E_d + E_{d1}) \tag{10}$$

where E_{d1} is the d-axis current prediction error at the last control instant.

Furthermore, based on (9) and (10), the expression of gain factor (k_1) can be obtained as

$$k_1 = \frac{-E_d \cdot L^2}{(T \cdot [R \cdot i_d(k) - u_d(k)] + E_d \cdot L)} \cdot \frac{2}{(E_d + E_{d1})} \tag{11}$$

where $u_d(k)$ represents the d-axis voltage in response to the optimal voltage vector. As a summary, Fig. 5 displays the diagram of parameter k_1 acquisition.

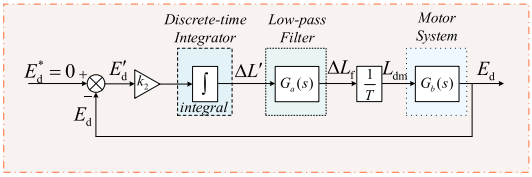

Fig. 6. Diagram of control structure in the motor system and inductance extraction algorithm.

2) Laplace Transform Simplification: Another way of calculation gain is the Laplace transform simplification method. For the purposes of obtaining the inductance information, a single closed-loop control structure for the current prediction error in the d-axis is constructed in Fig. 6. Obviously, the expected current prediction error in the d-axis (the input value) should be set as $E_d^* = 0$, and the feedback value is the actual current prediction error.

The difference between E_d and E_d^* is given by the following formula:

$$E_d' = E_d^* - E_d. \tag{12}$$

According to the forward Euler's theorem, the expression of the inductance information ($\Delta L'$) through the part of a discrete-time integrator is

$$\Delta L'(k) = \Delta L'(k-1) + T \cdot k_2 \cdot E_d' \tag{13}$$

where T stands for the control period. $\Delta L'(k)$ means the inductance information at the kth instant. $\Delta L'(k-1)$ refers to the information of inductance at the $(k-1)$th instant.

In addition, $G_a(s)$ means the transfer function of the low-pass filter. The equation of the low-pass filter is written as follows:

$$\Delta L_f(k) - \Delta L_f(k-1) = T \cdot [\Delta L' - \Delta L_f(k-1)] \tag{14}$$

where $\Delta L_f(k)$ and $\Delta L_f(k-1)$ stand for the inductance parameter obtained from the instant k and $k-1$, respectively. From (14), the expression of the low-pass filter under the time domain can be adapted as the following equation:

$$d\Delta L_f(t)/dt + \Delta L_f(t) = \Delta L'. \tag{15}$$

Therefore, the transfer function $G_a(s)$ can be obtained as

$$G_a(s) = \Delta L_f / \Delta L' = 1/(s+1). \tag{16}$$

Then, on the basis of the prediction error (7), the information about inductance is presented as

$$\Delta L_f = T \cdot [1/(L + \Delta L) - 1/L]. \tag{17}$$

Furthermore, according to (17), divided by the control period T, the inductance parameter information can be shown as

$$L_{dm} = \Delta L_f / T = [1/(L + \Delta L) - 1/L]. \tag{18}$$

Therefore, obtained inductance information form (18) can be used directly in the transfer function $G_b(s)$, which represents the actual motor system model.

According to (7) and (18), the transfer function $G_b(s)$ can be shown by

$$G_b(s) = E_d / L_{dm} = T \cdot [R \cdot i_d - u_d]. \tag{19}$$

Assume that the motor runs in the stable state; the current in the d-axis at kth instant can be seen as $i_d = 0$. And based on the d-axis voltage in (1), the transfer function $G_b(s)$ can be simplified as

$$G_b(s) = E_d / L_{dm} = -T \cdot u_d. \tag{20}$$

From the condition above $i_d = 0$, the result $di_d(t)/dt$ in (1) can be seen as $di_d(t)/dt = 0$. Therefore, (20) can be expressed by

$$G_b(s) = T\omega_e L_0 i_q \tag{21}$$

where L_0 stands for the actual inductance parameter of SPMSM.

In this article, the integral controller can be replaced by the transfer function, which is expressed as

$$G_I(s) = \Delta L'/(E_d^* - E_d) = k_i/s \tag{22}$$

where the gain k_i can be seen as the coefficient k_2 in Fig. 6.

According to (16), (21), and (22), the transfer function of an open loop in the whole system about inductance extraction is given by

$$G_{op}(s) = G_I(s) \cdot G_a(s) \cdot \frac{1}{T} \cdot G_b(s) = \frac{k_i \omega_e L_0 i_q}{s(s+1)}. \tag{23}$$

In addition, the feedback link in Fig. 6 can be substituted by the $H(s)$, whose gain is 1. Therefore, the transfer function can be figured out, which is expressed as

$$G_{cp}(s) = G_{op}(s)/[1 + G_{op}(s) \cdot H(s)] = k_{op}/\left(s^2 + s + k_{op}\right). \tag{24}$$

According to (23), the gain of the open-loop system is represented in the following equation:

$$k_{op} = k_i \cdot \omega_e \cdot L_0 \cdot i_q. \tag{25}$$

Then, based on (24), the feature equation of the closed loop in the system of inductance extraction is expressed as

$$s^2 + s + k_{op} = 0. \tag{26}$$

In addition, the typical expression for a second-order system can be rewritten by

$$s^2 + 2\xi\omega_n s + \omega_n^2 = 0. \tag{27}$$

Therefore, by comparing (26) and (27), the equivalent formula can be obtained as

$$\begin{cases} 2\xi\omega_n = 1 \\ \omega_n^2 = k_{op} \end{cases}. \tag{28}$$

According to the literature [23], [24], the damping ratio $\zeta = 0.707$ is designed to achieve the best response characteristic. Therefore, variables in (28) can be figured out as follows:

$$\begin{cases} \xi = \sqrt{2}/2 = 0.707 \\ \omega_n = 1/(2\xi) = \sqrt{2}/2 \\ k_{op} = \omega_n^2 = 1/2 \end{cases}. \tag{29}$$

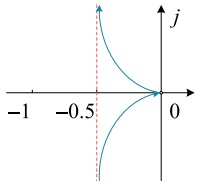

Fig. 7. Amplitude–phase characteristic curve of the open-loop system.

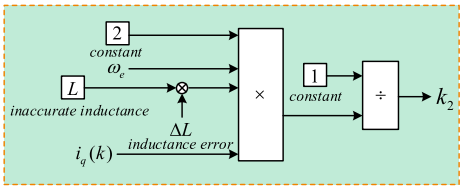

Fig. 8. Diagram of parameter k_2 acquisition.

Under the condition of (29), the amplitude–phase characteristic curve (polar diagram) of the open-loop system (23) is shown in Fig. 7.

According to the Nyquist stability criterion, Fig. 7 proves that the system of an open loop is maintaining stability. Therefore, the value of the variable k_{op} does not influence the system's stability.

Then, according to expressions (25) and (29), the gain factor (k_2) can be calculated by

$$k_i = k_2 = \frac{1}{2 \cdot [\omega_e \cdot (L + \Delta L) \cdot i_q(k)]}. \tag{30}$$

Therefore, the appropriate gain factor of integral parameter k_2 can be calculated online according to the system real-time state. And the diagram of parameter k_2 acquisition is shown in Fig. 8. Furthermore, under the control of the integral controller with gain k_2, it can be accomplished by obtaining the accurate inductance information L_{dm}. Then, according to the relationship expression (18) between L_{dm} and ΔL, the inductance error ΔL can be extracted as follows:

$$\Delta L = \left(-L^2 \cdot L_{dm}\right)/(L_{dm} \cdot L + 1). \tag{31}$$

Then, the inductance error ΔL can be used to update the current prediction model and substitute the information of the flux linkage, which is introduced in Section IV-B. Additionally, for the purpose of avoiding the adverse effects of high-frequency noise in the current prediction error E_d on the inductance extraction, this article applies an adaptive filtering method introduced in the literature [25]. On the other hand, in the actual application, ΔL in (30) at the kth instant is replaced by the inductance error value, which is extracted by the last control period, i.e., $(k-1)$th instant.

B. Flux-Linkage Substitution Algorithm

Based on the accurate inductance information obtained by the inductance extraction algorithm, a flux-linkage parameter substitution algorithm is proposed in this section.

According to (1), it is obvious that the flux-linkage information is only contained by the expression of u_q. Therefore, according to (1), the following formula can be used to express the flux-linkage information:

$$\psi_f(k) = \frac{u_q(k) - R \cdot i_q(k)}{\omega_e(k)} - L(k) \cdot \frac{i_q(k) - i_q(k-1)}{T \cdot \omega_e(k)} - L(k) \cdot i_d(k) \tag{32}$$

where $u_q(k)$ is the q-axis voltage of the optimal vector, which is selected from $(k-1)$th instant. The variables of $i_d(k)$ and $i_q(k)$ stand for the measured currents at kth instant. $i_q(k-1)$ indicates the current stored by the last instant. In addition, $L(k)$ represents the accurate inductance, which is given by

$$L(k) = L + \Delta L(k) \tag{33}$$

where $\Delta L(k)$ can be obtained from (31).

Then, based on (32), the flux-linkage information at kth, $(k-1)$th, and $(k-2)$th instants can be rewritten in the following way:

$$\begin{cases} \psi_f(k) = \frac{u_q(k) - R \cdot i_q(k)}{\omega_e(k)} - L(k) \frac{i_q(k) - i_q(k-1)}{T \cdot \omega_e(k)} \\ \quad -L(k) \cdot i_d(k) \\ \psi_f(k-1) = \frac{u_q(k-1) - R \cdot i_q(k-1)}{\omega_e(k-1)} - L(k-1) \frac{i_q(k-1) - i_q(k-2)}{T \cdot \omega_e(k-1)} \\ \quad -L(k-1) \cdot i_d(k-1) \\ \psi_f(k-2) = \frac{u_q(k-2) - R \cdot i_q(k-1)}{\omega_e(k-1)} - L(k-2) \frac{i_q(k-2) - i_q(k-3)}{T \cdot \omega_e(k-2)} \\ \quad -L(k-2) \cdot i_d(k-2) \end{cases}. \tag{34}$$

Additionally, when the motor running at its steady state, the electrical angular velocity of the motor in different instants can be seen as the same value, i.e., $\omega_e = \omega_e(k) = \omega_e(k-1) = \omega_e(k-2)$.

To enhance the accuracy of the result of the flux linkage, it needs to average the flux linkages at different control instants to obtain the final flux-linkage substitution expression. This means that the following expression can be obtained as:

$$f(L_{\psi_f}) = [\psi_f(k) + \psi_f(k-1) + \psi_f(k-2)]/3. \tag{35}$$

Substituting (34) into (35), we obtain

$$f(L_{\psi_f}) = (J - M - N)/3 \tag{36}$$

where J, M, and N are represented by (37) shown at the bottom of next page.

From (36) and (37), it is evident that the information of flux linkage can be expressed by the inductance information. It implies that this method can replace the parameter of flux linkage in the model of current prediction (2) with inductance parameter. Therefore, the predictive current model is able to be obtained without including the flux-linkage parameter as follows:

$$\begin{bmatrix} i_d^p(k+1) \\ i_q^p(k+1) \end{bmatrix} = \begin{bmatrix} i_d(k) & i_q(k) & u_d(k) & 0 \\ i_q(k) & -i_d(k) & u_q(k) & -1 \end{bmatrix} \cdot \begin{bmatrix} A & B & T/L & C \end{bmatrix}^T \tag{38}$$

where $A = 1 - TR/L$, $B = T\omega_e$, and $C = T\omega_e \cdot f(L_{\psi_f})/L$. In the actual application, a filter can be applied to further smooth the expression $f(L_{\psi_f})$. It is obvious from the prediction model

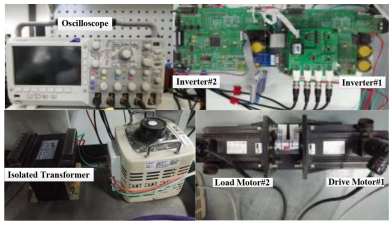

Fig. 9. Experimental platform of PMSM control system.

(38) that the accuracy of the predictive current model is predominantly decided by the parameter of inductance.

Summarizing, the proposed inductance extraction algorithm can be used together with the flux-linkage substitution algorithm to derive an exact current prediction model. Then, excellent control performance can be obtained even with the parameter mismatches. Therefore, the ability of antiparametric interference is improved.

V. Experimental Results

For the purpose of verifying the effectiveness of the proposed MPCC method in the case of mismatched parameters, the experiment is conducted and compared with the traditional MPCC approach. The control platform based on TMS320F28335 is utilized for implementing the experiment. The photograph of the experimental platform is illustrated in Fig. 9. In addition, the actual motor parameters applied to the experiment are provided in Table I.

In the experiments, the inductance parameter in the current prediction model of the proposed MPCC method can be changed by altering the value of the inductance parameter at the code composer studio (CCS) running interface. At the same time, the inductance parameter and flux-linkage parameter in the current prediction model of the conventional MPCC method can be simultaneously changed by altering the numeral of the flag bit at the CCS running interface.

From Fig. 10 to Fig. 13, the control performance in the proposed strategy is compared with that of the conventional method. Figs. 10 and 11 show the performance of both approaches when the mismatched inductance parameter occurs. Furthermore, Figs. 10(a) and 11(a) demonstrate that when the mismatch of inductance parameter occurs under the control of the traditional MPCC strategy, the current prediction error of the d-axis $[E_{d\text{-}ap}(k)]$ changes obviously. However, by the control of the proposed approach with two different integral gain calculations (k_1 obtained by *Inductance discretization calculation* and k_2 obtained by *Laplace transform simplification*), the inductance parameter (L) of the prediction model is corrected to its exact value, and the current error in prediction of the d-axis $[E_{d\text{-}ap}(k)]$ declines to 0 in a short time, as shown in Figs. 10(b), (c) and

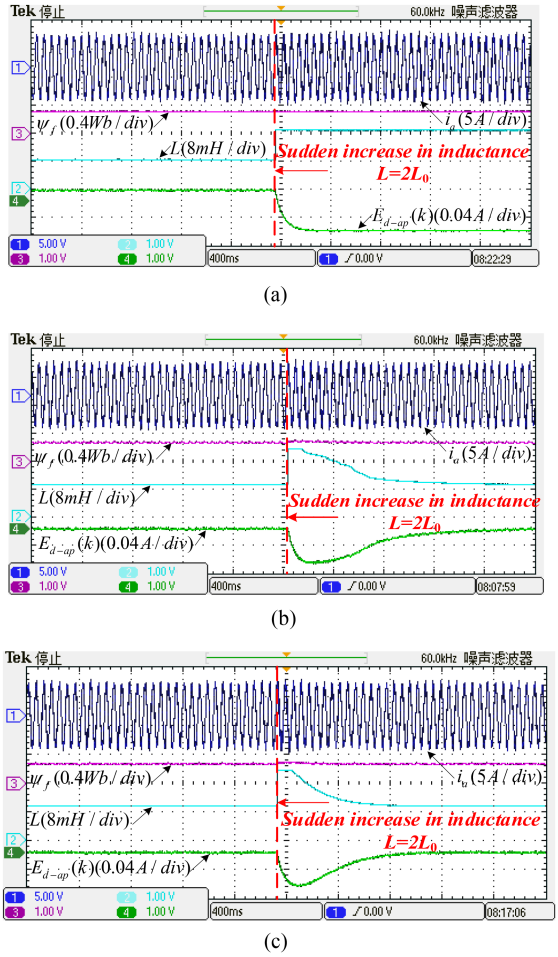

Fig. 10. Results of experiments in the conventional MPCC approach and the proposed MPCC approach when the parameter of inductance abruptly increases by 100% (With running speed of 500 r/min and loading torque of 5 N·m). (a) Sudden increase of 100% in the inductance parameter of the conventional MPCC method. (b) Sudden increase of 100% in the inductance parameter of the proposed MPCC method with k_1. (c) Sudden increase of 100% in the inductance parameter of the proposed MPCC method with k_2.

11(b), (c). On the other hand, it is obvious that the flux-linkage results obtained by the proposed method, as illustrated in Figs. 10 and 11, are stable and accurate. This proves that the algorithm for replacing the flux linkage with inductance information is correct and effective.

In addition, the current waveform and total harmonic distortion (THD) results are shown under the premise that the speed is 1000 r/min and the load torque is 5 N·m for the condition of inductance (L) changes.

From Figs. 12 and 13, it can be found that when the inductance parameters of predictive model increase, the control performance of the conventional MPC becomes bad. However, the

$$\begin{cases} J = \{u_q(k) + u_q(k-1) + u_q(k-2) - R \cdot [i_q(k) + i_q(k-1) + i_q(k-2)]\}/\omega_e(k) \\ S(n) = L(n) \cdot [i_q(n) - i_q(n-1)] \\ M = [S(k) + S(k-1) + S(k-2)]/[T \cdot \omega_e(k)] \\ N = L(k) \cdot i_d(k) + L(k-1) \cdot i_d(k-1) + L(k-2) \cdot i_d(k-2) \end{cases} \tag{37}$$

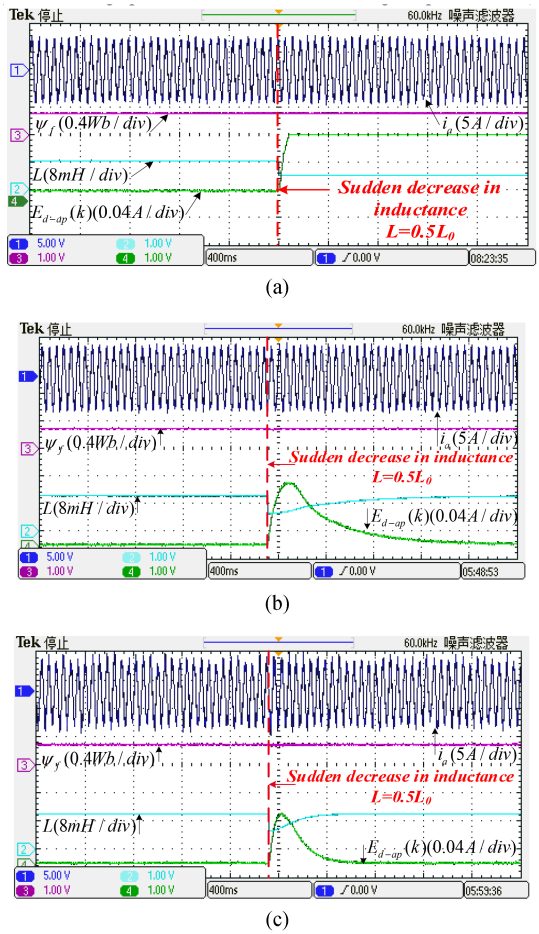

Fig. 11. Results of experiments in the traditional MPCC method and the proposed MPCC method when the parameter of inductance abruptly decreases by 50% (With running speed of 500 r/min and loading torque of 5 N·m). (a) Sudden decrease of 50% in the inductance parameter of the conventional MPCC method. (b) Sudden decrease of 50% in the inductance parameter of the proposed MPCC method with k_1. (c) Sudden decrease of 50% in the inductance parameter for the proposed MPCC strategy with k_2.

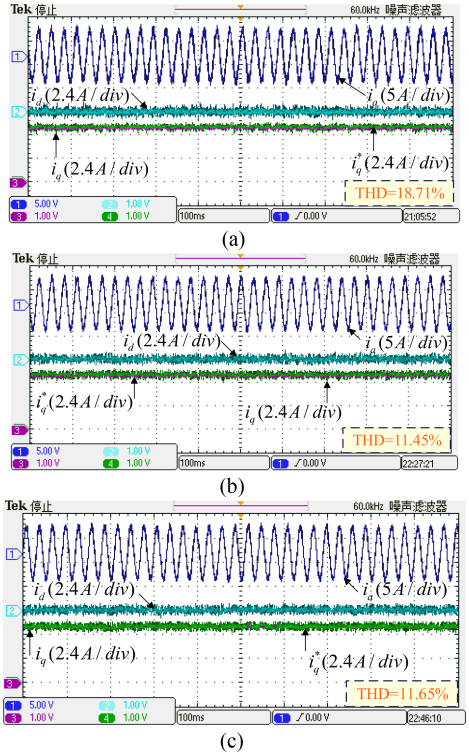

Fig. 12. Current waveform and THD results in the conventional MPCC approach and the proposed MPCC approach when a steady state is reached after a sudden 100% increase in the inductance parameter. (a) Conventional MPCC method. (b) Proposed MPCC method with k_1. (c) Proposed MPCC method with k_2.

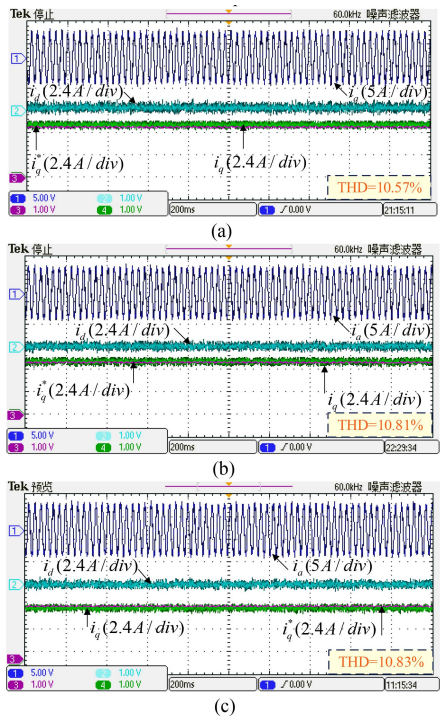

Fig. 13. Current waveform and THD results in the conventional MPCC approach and the proposed MPCC approach when a steady state is reached after a sudden 50% decrease in the inductance parameter. (a) Conventional MPCC method. (b) Proposed MPCC method with k_1. (c) Proposed MPCC method with k_2.

proposed method can eliminate the negative effect of parameter change.

In addition, in Figs. 14 and 15, a comparison of the dynamic property of the proposed strategy and that of the conventional strategy is shown when load torque abruptly increases from 3 to 5 N·m with the running speed of 1000 r/min and the parameter mismatches exist.

Fig. 14(a) illustrates the experimental results when the parameter of inductance (L) and flux linkage (ψ_f) applied to the prediction model suddenly increase under the control of the traditional MPCC method. According to the results, the static error between the reference current of the q-axis (i_q^*) and the actual current of the q-axis (i_q) is obvious, and the ripple of the phase current is large. Fig. 14(b) and (c) shows the different integral gain factors k_1 and k_2 used in the proposed method when the parameter of inductance decreases by 100%. It can be found that the worse current performance is improved effectively and the current error in the q-axis is eliminated, contrasted with the conventional method. Additionally, it is worth noting

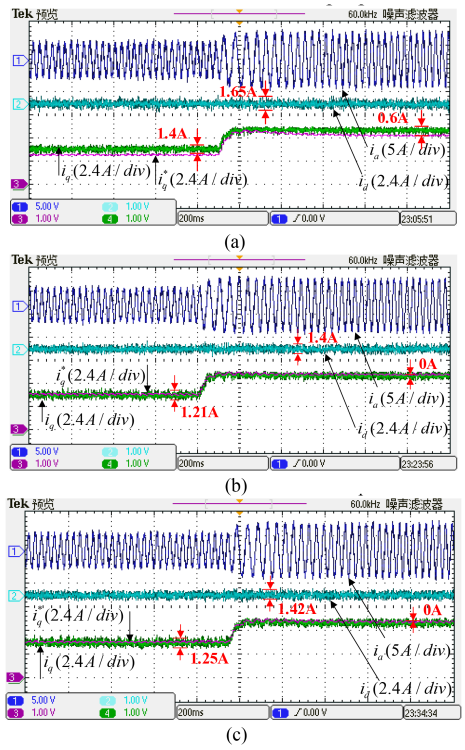

Fig. 14. Results of experiments in the conventional MPCC method and the proposed MPCC strategy when load torque abruptly increases (3–5 N·m) with the running speed of 1000 r/min. (a) Conventional MPCC method with mismatched parameter ($L = 2L_0$, $\psi_f = 2\psi_{f0}$). (b) Proposed MPCC method (k_1) with mismatched parameter ($L = 2L_0$). (c) Proposed MPCC method (k_2) with mismatched parameter ($L = 2L_0$).

TABLE II
COMPARISON OF ADVANTAGES AND DISADVANTAGES BETWEEN THE METHOD "INDUCTANCE DISCRETIZATION CALCULATION" AND THE METHOD "LAPLACE TRANSFORM SIMPLIFICATION"

	The designing progress	Reaction time	Number of variables that require additional storage
The method "*Inductance discretization calculation*"	*Simple*	*Longer*	2
The method "*Laplace transform simplification*"	*Complicate*	*Shorter*	1

that since the flux linkage in the proposed method is replaced by the inductance information, sudden changes in flux linkage in the conventional methods do not exist in the proposed method.

Fig. 15 illustrates the contradistinction between the traditional approach and the proposed approach in terms of control performance when both the inductance and flux-linkage parameters have been reduced by 50%. Similarly, it is apparent that the conventional method exists current error in the q-axis; however, the proposed method is capable of achieving optimized control performance.

In summary, the parameter mismatches of the prediction model can cause a serious effect on the traditional MPCC

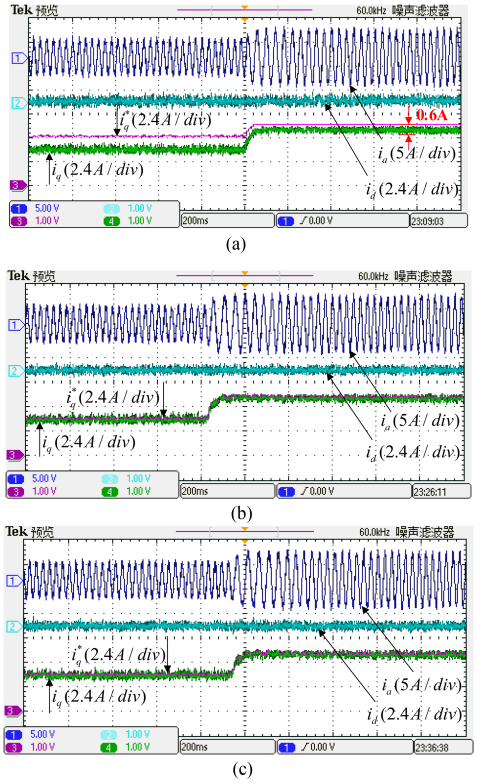

Fig. 15. Waveform of experiments in the conventional MPCC approach and the proposed MPCC approach when load torque abruptly increases (3–5 N·m) with the running speed of 1000 r/min. (a) Conventional MPCC method with mismatched parameter ($L = 0.5L_0$, $\psi_f = 0.5\psi_{f0}$). (b) Proposed MPCC method (k_1) with mismatched parameter ($L = 0.5L_0$). (c) Proposed MPCC method (k_2) with mismatched parameter ($L = 0.5L_0$).

method in terms of control performance. In contrast, in this article, the proposed MPCC approach can restrain the negative influence of the parameter mismatch effectively. Additionally, the proposed two gain design methods can achieve satisfactory control performance.

According to the experimental results, as shown in Figs. 10–15, (11), and (30), the advantages and disadvantages of the two proposed methods in this article are shown as follows.

1) The advantage of the method *Inductance discretization calculation* is only that it contains the inductance parameter which input into the current prediction model and the design process is relatively simple.
2) The disadvantage of the method *Inductance discretization calculation* is that its reaction time is long and more data need to be additionally stored.
3) The advantage of the method *Laplace transform simplification* is only one datum needs to be stored additionally and the reaction time is short.
4) The disadvantage of the method *Laplace transform simplification* is the design process, which is more complicated.

Table II lists the advantages and the disadvantages of the method *Inductance discretization calculation* and the method *Laplace transform simplification*. Thus, the corresponding method can be selected according to the actual system requirements.

VI. Conclusion

For the purpose of alleviating the influence caused by the parameter mismatches of the prediction model on the SPMSM control system, a robust MPCC strategy was proposed in this article. In this article, the principal contributions were as follows.

1) Using the error in the current prediction of the *d*-axis, a simple inductance extraction algorithm and two kinds of parameter design methods were presented. And the method *Inductance discretization calculation* had its own advantage in simple designing progress, but a longer reaction time was the disadvantage of this method. On the other hand, the method *Laplace transform simplification* had its own advantage in the shorter reaction time and its own disadvantage on the moment of inductance value substituted into the coefficient formula was not the current operating moment.
2) The flux-linkage parameter in the current prediction model can be eliminated by the extracted inductance of different control instants. Finally, the results of the experiment prove that the proposed method can strengthen the parameter robustness of the MPC system. This illustrates that the proposed strategy enhances the robustness of parameters while maintaining the simple control structure.

References

[1] Z. Qiao, T. Shi, Y. Wang, Y. Yan, C. Xia, and X. He, "New sliding-mode observer for position sensorless control of permanent-magnet synchronous motor," *IEEE Trans. Ind. Electron.*, vol. 60, no. 2, pp. 710–719, Feb. 2013.

[2] W. Liang, W. Fei, and P. C.-K. Luk, "An improved sideband current harmonic model of interior PMSM drive by considering magnetic saturation and cross-coupling effects," *IEEE Trans. Ind. Electron.*, vol. 63, no. 7, pp. 4097–4104, Jul. 2016.

[3] J. Yang, W.-H. Chen, S. Li, L. Guo, and Y. Yan, "Disturbance/uncertainty estimation and attenuation techniques in PMSM drives—A survey," *IEEE Trans. Ind. Electron.*, vol. 64, no. 4, pp. 3273–3285, Apr. 2017.

[4] J. Lara, J. Xu, and A. Chandra, "Effects of rotor position error in the performance of field-oriented-controlled PMSM drives for electric vehicle traction applications," *IEEE Trans. Ind. Electron.*, vol. 63, no. 8, pp. 4738–4751, Aug. 2016.

[5] Y. Zhang and J. Zhu, "Direct torque control of permanent magnet synchronous motor with reduced torque ripple and commutation frequency," *IEEE Trans. Power Electron.*, vol. 26, no. 1, pp. 235–248, Jan. 2011.

[6] W. Chen, S. Zeng, G. Zhang, T. Shi, and C. Xia, "A modified double vectors model predictive torque control of permanent magnet synchronous motor," *IEEE Trans. Power Electron.*, vol. 34, no. 11, pp. 11419–11428, Nov. 2019.

[7] F. Mendoza-Mondragón, V. M. Hernández-Guzmán, and J. Rodríguez-Reséndiz, "Robust speed control of permanent magnet synchronous motors using two-degrees-of-freedom control," *IEEE Trans. Ind. Electron.*, vol. 65, no. 8, pp. 6099–6108, Aug. 2018.

[8] Q. Liu and K. Hameyer, "Torque ripple minimization for direct torque control of PMSM with modified FCSMPC," *IEEE Trans. Ind. Appl.*, vol. 52, no. 6, pp. 4855–4864, Nov./Dec. 2016.

[9] Z. Mynar, L. Vesely, and P. Vaclavek, "PMSM model predictive control with field-weakening implementation," *IEEE Trans. Ind. Electron.*, vol. 63, no. 8, pp. 5156–5166, Aug. 2016.

[10] X. Zhang, Y. Cheng, Z. Zhao, and K. Yan, "Optimized model predictive control with dead-time voltage vector for PMSM drives," *IEEE Trans. Power Electron.*, vol. 36, no. 3, pp. 3149–3158, Mar. 2021.

[11] X. Zhang and B. Hou, "Double vectors model predictive torque control without weighting factor based on voltage tracking error," *IEEE Trans. Power Electron.*, vol. 33, no. 3, pp. 2368–2380, Mar. 2018.

[12] J. Rodriguez *et al.*, "State of the art of finite control set model predictive control in power electronics," *IEEE Trans. Ind. Informat.*, vol. 9, no. 2, pp. 1003–1016, May 2013.

[13] X. Zhang, K. Yan, and M. Cheng, "Two-stage series model predictive torque control for PMSM drives," *IEEE Trans. Power Electron.*, vol. 36, no. 11, pp. 12910–12918, Nov. 2021.

[14] H. A. Young, M. A. Perez, and J. Rodriguez, "Analysis of finite-control-set model predictive current control with model parameter mismatch in a three-phase inverter," *IEEE Trans. Ind. Electron.*, vol. 63, no. 5, pp. 3100–3107, May 2016.

[15] X. Zhang, B. Hou, and Y. Mei, "Deadbeat predictive current control of permanent-magnet synchronous motors with stator current and disturbance observer," *IEEE Trans. Power Electron.*, vol. 32, no. 5, pp. 3818–3834, May 2017.

[16] M. Yang, X. Lang, J. Long, and D. Xu, "Flux immunity robust predictive current control with incremental model and extended state observer for PMSM drive," *IEEE Trans. Power Electron.*, vol. 32, no. 12, pp. 9267–9279, Dec. 2017.

[17] Y. Jiang, W. Xu, C. Mu, and Y. Liu, "Improved deadbeat predictive current control combined sliding mode strategy for PMSM drive system," *IEEE Trans. Veh. Technol.*, vol. 67, no. 1, pp. 251–263, Jan. 2018.

[18] X. Zhang, L. Zhang, and Y. Zhang, "Model predictive current control for PMSM drives with parameter robustness improvement," *IEEE Trans. Power Electron.*, vol. 34, no. 2, pp. 1645–1657, Feb. 2019.

[19] Y. Li, Yong Li, and Q. Wang, "Robust predictive current control with parallel compensation terms against multi-parameter mismatches for PMSMs," *IEEE Trans. Energy Convers.*, vol. 35, no. 4, pp. 2222–2230, Dec. 2020.

[20] X. Yuan, S. Zhang, C. Zhang, A. Galassini, G. Buticchi, and M. Degano, "Improved model predictive current control for SPMSM drives using current update mechanism," *IEEE Trans. Ind. Electron.*, vol. 68, no. 3, pp. 1938–1948, Mar. 2021.

[21] Y. Shi, K. Sun, L. Huang, and Y. Li, "Online identification of permanent magnet flux based on extended Kalman filter for IPMSM drive with position sensorless control," *IEEE Trans. Ind. Electron.*, vol. 59, no. 11, pp. 4169–4178, Nov. 2012.

[22] K. Liu, Z. Q. Zhu, and D. A. Stone, "Parameter estimation for condition monitoring of PMSM stator winding and rotor permanent magnets," *IEEE Trans. Ind. Electron.*, vol. 60, no. 12, pp. 5902–5913, Dec. 2013.

[23] X. Zhang, Z. Zhao, Y. Cheng, and Y. Wang, "Robust model predictive current control based on inductance and flux linkage extraction algorithm," *IEEE Trans. Veh. Technol.*, vol. 69, no. 12, pp. 14893–14902, Dec. 2020.

[24] M. Sun, J. Zhou, B. Dong, S. Zheng, and T. Wen, "Nutation mode suppression of magnetically levitated turbo-rotor via damping optimization," *IEEE Trans. Ind. Electron.*, vol. 68, no. 12, pp. 12607–12614, Dec. 2021.

[25] A. Rosado-Muñoz, M. Bataller-Mompeán, E. Soria-Olivas, C. Scarante, and J. F. Guerrero-Martínez, "FPGA implementation of an adaptive filter robust to impulsive noise: Two approaches," *IEEE Trans. Ind. Electron.*, vol. 58, no. 3, pp. 860–870, Mar. 2011.

Xiaoguang Zhang (Senior Member, IEEE) received the B.S. degree from the Heilongjiang Institute of Technology, Harbin, China, in 2007, and the M.S. and Ph.D. degrees from the Harbin Institute of Technology, Harbin, in 2009 and 2014, respectively, all in electrical engineering.

From 2012 to 2013, he was a Research Associate with Wisconsin Electric Machines and Power Electronics Consortium, University of Wisconsin–Madison, Madison, WI, USA. He has authored or coauthored more than 70 technical papers in the area of motor drives. He is currently a Distinguished Professor with the North China University of Technology, Beijing, China, and the Director of Beijing Power Electronics and Electrical Transmission Engineering Research Center. His current research interests include power electronics and electric machines' drives.

Dr. Zhang is an Associate Editor for *IET Power Electronics*.

Ziwei Wang was born in Hebei, China, in 1996. He received the B.S. degree in electrical engineering from the North China University of Science and Technology, Qinhuangdao, China, in 2019. He is currently working toward the M.S. degree in electrical engineering with the North China University of Technology, Beijing, China.

The main research direction during his master's degree is the control of permanent magnet synchronous motor, including model predictive control and robust control.